Int. J. Dev. Biol. 44: 757-768 (2000)

Original Article

Temporospatial patterns of apoptosis in chick embryos during the morphogenetic period of development

MASASHI HIRATA* and BRIAN K. HALL

Department of Biology, Dalhousie University, Halifax, Nova Scotia, Canada

ABSTRACT We examined the temporospatial pattern of naturally occurring apoptosis in chick embryos to five days of incubation (H.H. stages 1-25; Hamburger and Hamilton, 1951) using TUNEL labeling. The initial TUNEL-positive structure was the embryonic shield at stage 1. Apoptotic cells became ubiquitously present within embryos by stage 3, which is early in gastrulation. Until stage 6, TUNEL-positive cells were restricted to the headfold region. In embryos of stages 7-8, most cell death was localized at the most anterior neural plate. TUNEL-positive neural plate, notochord and somites appeared at stage 9. Otic and optic regions became TUNEL-positive at stage 11. The aggregation of cells from which the tail bud arises contains apoptotic cells from stage 11 onwards. At stage 16, scattered TUNEL-positive cells appeared in the branchial arches. Three streams of apoptotic neural crest cells in the cranial region became most clearly visible at stage 18. The secondary neural tube from which caudal structures develop contains apoptotic cells at stage 14. Apoptotic cells are present in the branchial arches and lateral body wall for extended periods, stages 16-25 and 25 respectively. At stages 24-25, intense positive regions of cell death were confined to the caudal regions of the arches, to limb and tail buds and to the lateral body wall, the latter in relation to body wall closure. The new findings in this study are discussed along with past studies to provide the temporospatial pattern of cell death during early chick development.

KEY WORDS: *chick development, programmed cell death (apoptosis), TUNEL labeling, sclerotome, somites, neural crest.*

Introduction

Programmed cell death (apoptosis), the most common form of eukaryotic cell death, is a normal physiological phenomenon known to play an important role in morphogenesis associated with normal embryonic development in both vertebrates and invertebrates (Glücksmann, 1951; Clarke, 1990; Ellis *et al.*, 1991; Jacobson *et al.*, 1997). Apoptosis serves multiple functions during development, including: removal of damaged, misplaced, abnormal or excess cells; sculpting structures during morphogenesis; removal of structures as during metamorphosis; controlling cell number; and removing cells that establish inappropriate connections or that are improperly induced. Generally, cells undergoing apoptosis display characteristic features of membrane blebbing, nuclear and cytoplasmic shrinkage, chromatin condensation and DNA fragmentation (Kerr *et al.*, 1972). DNA fragmentation can be detected *in situ* using the TUNEL (Terminal deoxynucleotidyl transferase mediated dUTP Nick End Labeling) method developed by Gavrieli *et al.* (1992). The TUNEL method is routinely used as a technique to detect apoptotic cells *in situ*, either in whole embryos or in tissue sections.

A detailed analysis of patterns of programmed cell death in entire embryos throughout early development has been reported

Abbreviations used in this paper: ANZ, anterior necrotic zone; BA1, first branchial arch (third pharyngeal arch); BSA, bovine serum albumen; CF, choroid fissure; DA, dorsal aorta; DC, diencephalon; DM, dermomyotome; DNase I, deoxyribonuclease; dUTP, deoxyuridine-5'-triphosphate; EC, ectoderm; EN, endoderm; FB, forebrain; FLB, forelimb bud; FR, the presumptive facial nerve (cranial nerve VII) root ganglion; GS, the presumptive glossopharyngeal nerve (cranial nerve IX) superior ganglion; H.H., Hamburger-Hamilton stages; HLB, hindlimb bud; HNK, human natural killer antigen; HY, hyoid arch (second pharyngeal arch); LS, lens sac; LV, lens vesicle; ME, mesoderm; MN, mandibular arch (first pharyngeal arch); MX, maxillary arch (first pharyngeal arch); NA, nasal pit; NF, neural fold; NO, notochord; NP, neural plate; NT, neural tube; OCI, inner layer of optic cup; OCO, outer layer of optic cup; OT, otic vesicle; PB, pineal body; PBS, phosphate-buffered saline; PBST, phosphate buffered saline with Triton; PBTL, phosphate buffered saline with Triton and levamisole; PFA, paraformaldehyde; PNT, primary neural tube; PNZ, posterior necrotic zone; r3, r4, r5, rhombomeres 3, 4 and 5; SCL, sclerotome; SNT, secondary neural tube; SO, somite; SP, segmental plateTdT, terminal deoxynucleotidyl transferase; TUNEL, Terminal deoxynucleotidyl transferase mediated dUTP Nick End Labeling.

***Address correspondence to:** Masashi Hirata. Department of Biology. Dalhousie University, Halifax NS Canada B3H 4J1. FAX: 902 494 3736.
e-mail: mhirata@is.dal.ca

0214-6282/2000/$20.00

Printed in Spain
www.ehu.es/ijdb

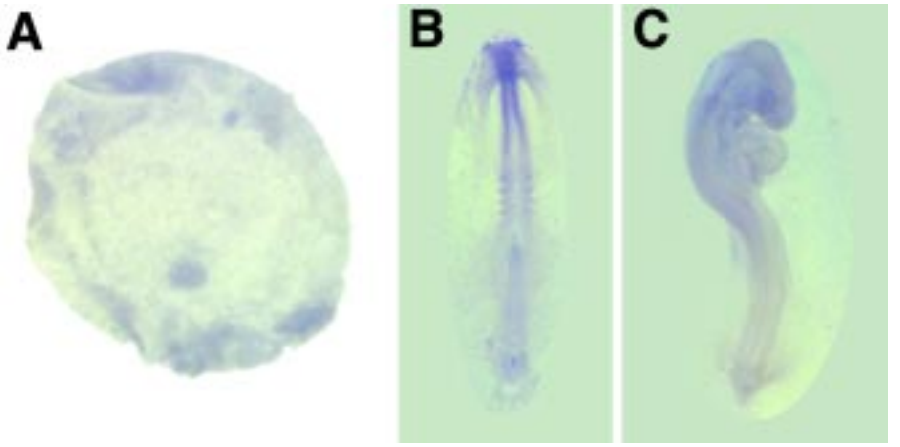

Fig. 1. Negative controls for whole-mount TUNEL staining at three representative embryonic stages. *Anterior is to the top.* **(A)** *H.H. stage 0 (unincubated egg).* **(B)** *H.H. stage 8 (4 pairs of somites).* **(C)** *H.H. stage 18 (33 pairs of somites). No TUNEL-positive staining was observed in these embryos.*

for only one vertebrate, *Xenopus*, in which cell death is first seen during gastrulation (Anderson *et al.,* 1997; Stack and Newport, 1997; Hensey and Gautier, 1997) and then especially evident in the developing neural tube, tail and sense organs (Hensey and Gautier, 1997). In the newt, *Cynops pyrrhogaster*, the first cell death also appears during gastrulation (Imoh, 1986). In *Xenopus*, the cell death seen during gastrulation represents activation by fertilization of a maternal program (Hensey and Gautier, 1997). Considerable cell death also accompanies metamorphosis in *Xenopus* (Nishikawa and Hayashi, 1995).

Although there are many studies on cell death in embryonic chicks (one of the most commonly used experimental animals in developmental biology), most of these studies have focused on individual organ systems during small windows of developmental time — limb buds (Saunders *et al.,* 1962; Hurle *et al.,* 1995; Lee *et al.,* 1999 and references therein), heart (Pexieder, 1975), tail bud (Schoenwolf, 1981; Sanders *et al.*, 1986; Miller and Briglin, 1996), sclerotome (Sanders, 1997) and neural crest (Lumsden *et al.,* 1991; Jeffs *et al.,* 1992; Jeffs and Osmond, 1992; Homma *et al.,* 1994; Farlie *et al.*, 1999; Lawson *et al.*, 1999). Although these studies provide windows through which to view cell death in individual tissues or organs, no past analysis reports the global temporospatial patterns of programmed cell death in chick embryos throughout the entire early morphogenetic period. Indeed, no amniote has been the subject of such an analysis.

We undertook a temporospatial analysis of naturally occurring cell death during the morphogenetic period of embryonic development (0-5 days of incubation, H.H. stages 1-25; Hamburger and Hamilton, 1951) using the TUNEL labeling technique on both whole mount and serially sectioned embryos. Immunostaining with the HNK-1 antibody was used to verify the neural crest origin of some TUNEL-positive cells. Although ours is the first global analysis of the temporospatial patterns of cell death during chick development (and only the second for any vertebrate), some of the areas of cell death we identify have been described before, although not in the context of global temporospatial patterns. In addition to the global temporospatial pattern of cell death, new data added from our study include: onset of cell death before gastrulation; apoptosis in the head fold and entire body axis at stages 6 and 8 respectively; cell death in the primordium of the tail bud at stage 11 and during secondary neurulation at stage 14; apoptosis in three streams of migrating cranial neural crest cells at stage 18; and extended periods of cell death in both the branchial (pharyngeal) arches and the body wall at stages 16-25 and 25 respectively. These new data, coupled with our data supporting or enhancing past studies, allow us to present the first integrated scenario for temporospatial patterns of cell death during differentiation, growth and morphogenesis in early chick embryogenesis.

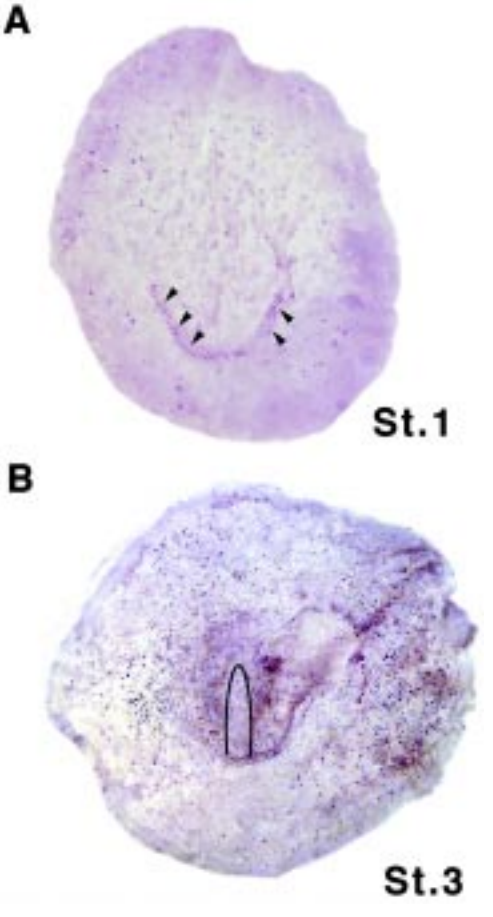

Fig. 2. Apoptotic cells as detected by whole-mount TUNEL staining to primitive streak formation. *(A, B) Whole-mount stained embryos. Anterior is to the top.* **(A)** *Embryo of H.H. stage 1 (St. 1): TUNEL-positive cells in the embryonic shield (arrowheads).* **(B)** *Embryos of stage 3. Curved lines indicate the primitive streak. Anterior is to the top. The numbers of TUNEL-positive cells is dramatically increased.*

Results

Controls

No TUNEL-positive cells were observed in embryos in which the TUNEL reaction mixture was substituted by PBTL (negative controls). Negative controls at three representative developmental stages are shown in Fig. 1A-C. As a positive control, we treated embryos with DNase I to induce DNA strand breaks. TUNEL-positive cells were observed throughout the entire embryo (data not shown).

The period until primitive streak formation (0-20 hours of incubation; H.H. stages 1-3)

The first structure observed as TUNEL-positive was the embryonic shield at H.H. stage 1 (Fig. 2A), around 3 hours after the onset of incubation. TUNEL-positive cells were more ubiquitously observed within embryos except in the region of the primitive streak at H.H. stage 3 corresponding to about 10 hours after onset of incubation (Fig. 2B).

From head-process to early somitogenesis (20 hours-1.5 days of incubation; H.H. stages 5-9)

In embryos at the head-process stage (H.H. stages 5 to 6) TUNEL-positive cells were restricted to the anterior region where head fold formation would occur at H.H. stage 6 (Fig. 3A). At H.H. stages 7 to 8 (1-4 pairs of somites) much of the staining was localized to the anteromost edge of the neural plate in the future forebrain (Fig. 3 B,E). TUNEL-positive cells were also thinly scattering in the posterior open neural plate (Fig. 3B). A TUNEL-positive neural tube (neural plate) was first observed at H.H. stage 9 (7 pairs of somites, Fig. 3C). Analysis of histological sections confirmed that positive cells lay within the neural plate and in the epithelium adjacent to the neural plate, consistent with a role in folding of the neural tube (Fig. 3F). TUNEL-positive cells were scattered over the somitic region (Fig. 3F) and notochord (Fig. 3 D,F). The anterior intestinal portal also first became TUNEL-positive at stage 9 (Fig. 3D). This weak staining in the anterior intestinal portal became strongest at H.H. stage 14 (Fig. 4D) and then disappeared.

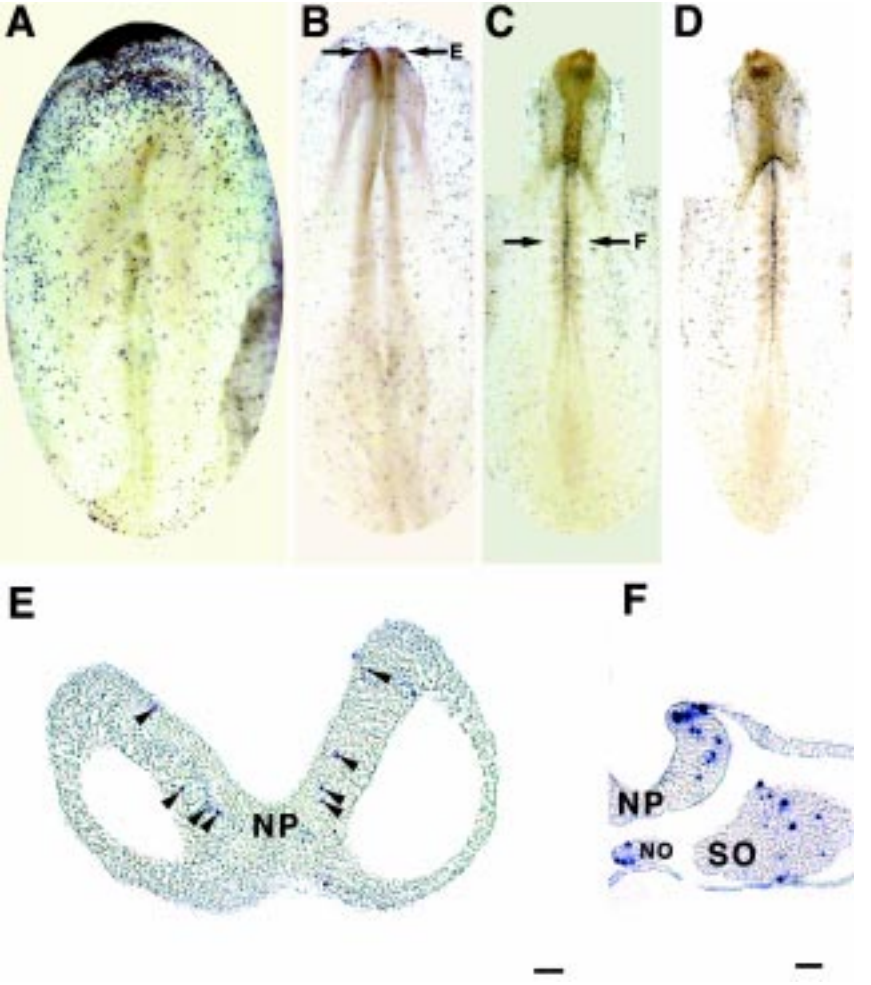

Fig. 3. Apoptotic cells detected between the head-process stage and early somitogenesis. *(A-D) Whole-mount-stained embryos of H.H. stage 5* **(A)**, *8* **(B)** *and 9* **(C)**, *dorsal view;* **(D)**, *ventral view). Anterior is to the top. (E, F) Transverse sections of TUNEL-stained embryos of H.H. stage 8* **(E)**, *(arrows in B) and 9* **(F)**, *(arrows in C). Most TUNEL-positive cells (arrowheads in E) are located in the neural plate of the future forebrain at stage 8. TUNEL-positive cells are seen within the neural plate, epidermis adjacent to the neural plate, somites and notochord at stage 9 (F). Scale bars, 20 μm.*

Mid somitogenesis (1.5-2 days of incubation; H.H. stages 11-14)

Otic and optic regions first became TUNEL-positive at H.H. stage 11 (13 pairs of somites). Staining of the optic region was faint (Fig. 4A) until H.H. stage 16.

Fore-, mid- and hindbrain are TUNEL-positive (Fig. 4A). TUNEL-positive cells in the forebrain are localized to the anterior forebrain with the exception of the optic region (Fig. 4 A,B). Cell death was observed in the rhombencephalon at this stage except at the level of the 4th rhombomere (Fig. 4A). This non-TUNEL-positive population coincided with a population of HNK-1-immunoreactive neural crest cells (Fig. 5A).

In the anterior trunk, TUNEL-positive cells were seen in the anteromost portion of the heart where the outflow tract connects to the pharynx (Fig. 4B). Neural tube and somitic regions were TUNEL positive (Fig. 4A). As seen in histological sections, notochord, somites, dorsal epithelium, neural tube and adjacent epithelium were TUNEL positive. TUNEL-positive cells within the neural tube were localized relatively more dorsally than in the previous stage. Occasionally, TUNEL-positive mesenchymal cells were seen associated with the neural tube in the most anterior trunk region at the level of somites 1-3 (Fig. 4E). Sometimes, TUNEL-positive cells in the notochord co-localized with the positive cells in the floor plate of the neural tube (Fig. 4E). TUNEL-positive cells within somites tend to be restricted to the ventral region (Fig. 4E) in comparison with the previous stage. A TUNEL-positive cell population is found in the most caudal region of embryos at H.H. stage 11 (Fig. 4C). During H.H. stages 11-14, apoptotic cells were observed in relation to closure of the neural tube (Fig. 4C). Transverse histological sections just posterior to the level of neural tube closure revealed that positive cells were distributed in the dosalmost neural fold and adjacent epithelium

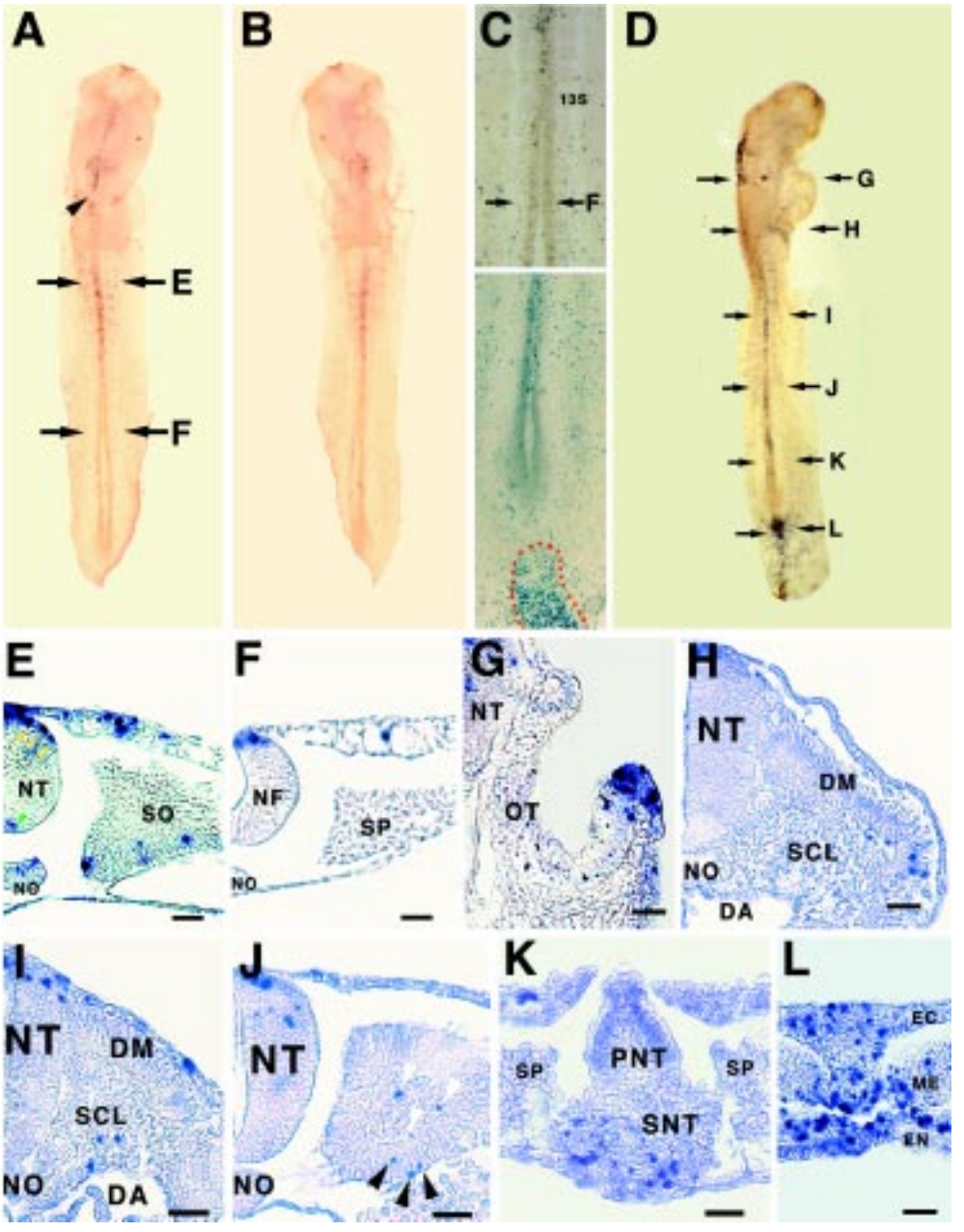

Fig. 4. Apoptotic cells as detected at mid somitogenesis. *(A-D) Whole-mount-stained embryos.* **(A)** *Stage 11, dorsal view. An arrowhead indicates the 4th rhombomere level, apoptotic cells being seen in r3 and r5 but not in r4.* **(B)** *Stage 11, ventral view.* **(C)** *Stage 11, higher magnification of A to show neural tube closure posterior to the last somite (13S, upper) and the caudalmost embryonic region (lower). Red dots outline TUNEL-positive cells.* **(D)** *Stage 14, dorsal view. Arrows indicate the level of the transverse sections shown in (G-L). (E-L) Transverse sections of TUNEL-stained embryos. (E, F) Stage 11.* **(E)** *Anterior trunk region at the 3-somite-level as indicated in (A). Neural tube, notochord, somites, dorsal epidermis, neural tube and adjacent epidermis are TUNEL positive. Yellow arrowheads show TUNEL-positive neural crest cells associated with the neural tube. Blue and green arrowheads show TUNEL-positive cells in the notochord and the floor plate respectively.* **(F)** *Just posterior to neural tube closure as indicated in (A) and (C). (G-L) Stage 14.* **(G)** *At the otic level.* **(H)** *Anterior trunk region as indicated in (D).* **(I)** *Mid trunk region as indicated in (D).* **(J)** *Posterior trunk at the level of somite 19. TUNEL-positive cells in the somitocoele (white arrowheads) and epithelial wall (black arrowheads) of early somites.* **(K)** *Unsegmented caudal trunk region as indicated in (D). TUNEL-positive cells are observed within the developing secondary neural tube.* **(L)** *Caudalmost tail region as indicated in (D). All three germ layers contain TUNEL-positive cells. Scale bars, 20 μm.*

(Fig. 4F). More TUNEL-positive cells were present in the neural tube than at earlier stages and the region of cell death widened along the rostro-caudal axis until H.H. stage 14, indicating an increasingly important role for cell death in neural development over time.

At H.H. stage 14 (22 pairs of somites), staining of the mesencephalic region became relatively faint compared to the previous stage, although the rhombencephalic region was strongly TUNEL positive. The otic region was strongly TUNEL positive, while the optic region remained weakly TUNEL positive (Fig. 4D). Histological sections revealed TUNEL-positive cells in the otic region distributed at the boundary of the ventral otic placode and epidermis where invagination of the otic placode is taking place (Fig. 4G).

In the trunk, the dorsal neural tube, somitic region and tail bud were TUNEL positive. A scattering of TUNEL-positive cells was observed mainly in the sclerotomal region at H.H. stage 14 (Fig. 4I). However, in the most anterior trunk, dermomyotome also contained small numbers of TUNEL-positive cells (Fig. 4H). In the caudal trunk, a thin scattering of TUNEL-positive cells was observed in both the somitocoele and epithelial walls of early somites (Fig. 4J).

In the caudal trunk at this stage, the developing secondary neural tube was observed ventral to the primary neural tube. In this region of overlapping primary and secondary neural tube, the developing secondary neural tube contained many more TUNEL-positive cells than did the primary neural tube at the same axial level (Fig. 4K). TUNEL-positive cells within the developing secondary neural tube did not show clear localization along the dorso-ventral axis when compared with the pattern in the developing primary neural tube (Fig. 4K). The tail bud region also became

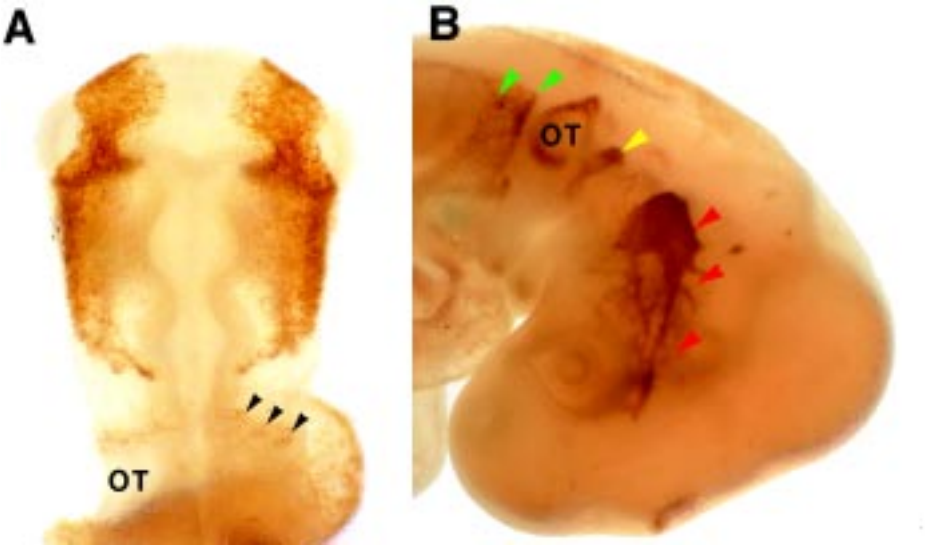

Fig. 5. HNK-1-immunoreactive neural crest cells detected in the cranial region of whole-mount-stained embryos of stage 11 (A) and 18 (B). (A) *H.H. stage 11, dorsal view. Anterior is to the top. HNK-1-immunoreactive neural crest cells are not visible at the level of rhombomere 3. Small numbers of preotic HNK-1-immunoreactive neural crest cells (arrowheads) are visible anterior to the otic vesicle (r4) level.* **(B)** *H.H. stage 18, lateral view. Anterior is to the right. Three HNK-1-immunoreactive populations of neural crest-derived ganglionic precursors are seen at identical locations to the anterior (red arrowheads), preotic (yellow arrowhead) and postotic (green arrowheads) streams of TUNEL-positive cells respectively (cf. Fig. 6D).*

definitely and strongly TUNEL-positive at this stage (Fig. 4D). Histological sections through the tail bud revealed densely scattering TUNEL-positive cells in all three germ layers (Fig. 4L). Staining in the tail bud region was continuously observed from this stage until H.H. stage 25. The number of TUNEL-positive cells within the notochord was sharply reduced at H.H. stage 14.

Late somitogenesis (2-3 days of incubation; H.H. stages 16-18)

At stage 16 (27 pairs of somites) staining of the cranial neural tube became relatively faint compared to the previous stages. TUNEL-staining of the optic region became clearly visible. Foci of TUNEL-positive cells were observed in two portions in the eye (Fig. 6A). Histological sections revealed that both were associated with sites of invagination: one at the boundary between inner and outer layer of the optic cup; the other at the dorsal folding of the invaginating lens primordium (Fig. 6E). This pattern reproducibly continued until H.H. stage 20, when the pattern changed. Otic regions were still TUNEL positive as at H.H. stage 14. Scattered TUNEL-positive cells were first observed in the branchial arches at H.H. stage 16 (Fig. 6C). In the trunk, dermomyotome and ventral sclerotome were TUNEL-positive (Fig. 6F). Both dorsal neural tube with adjacent epithelium and mesenchymal cells around the dorsal neural tube were TUNEL-positive as at previous stages (data not shown).

At H.H. stage 18 (33 pairs of somites), programmed cell death was frequently observed in the neural tube, branchial, otic, somitic regions and eyes (Fig. 6 B,D). Three streams of TUNEL-positive cells were clearly visible in the cranial region at H.H. stage 18 (Fig. 6D). The most anterior population originated from the forebrain and midbrain extending towards the anterior branchial (mandibular) arches (Fig. 6 D,I). Sectional analysis revealed TUNEL-positive mesenchymal cells scattering within the branchial arches (Fig. 6J). Another TUNEL-positive stream was seen in the preotic region, extending from the anterior rhombencephalic region towards the hyoid arches (Fig. 6 D,K). The most caudal stream-like population was observed at the postotic region, and seemed to be directed to the posterior branchial arches (Fig. 6D). The position of these three streams was identical to three HNK-1-immunoreactive populations of ganglionic precursors in the cranial region at this stage (Fig. 5B). Parahorizontal histological sections through the ventral otic vesicle revealed TUNEL-positive cells in the postotic and preotic stream at the sites of the root ganglion of the facial nerve (cranial nerve VII) and the superior ganglion of glossopharyngeal nerve (cranial nerve IX) (Fig. 6K). Weakly TUNEL-positive nasal pit and pineal body were also observed at this stage (Fig. 6 G,H), with the staining in the nasal pit continuing to H.H. stage 25.

In the anterior to mid-trunk, TUNEL-positive-dermomyotome, dorsal neural tube with adjacent epithelium (Fig. 6L), ventral sclerotome (Fig. 6 L,N), and mesenchymal cells around the dorsal neural tube (Fig. 6 L,M) were observed as in previous stages. Some TUNEL-positive mesenchymal cells around the dorsal neural tube appeared to be streaming into the dorsal sclerotome (Fig. 6M). In the anterior trunk, a TUNEL-positive band was observed as a continuation of the postotic stream (Fig. 6 B,D). Histological sections revealed TUNEL-positive dermomyotome and associated mesenchymal cell mass in the ventro-lateral portion of the somite (Fig. 6L). Almost no TUNEL-positive cells were seen within the notochord, except in the most caudal trunk at stage 16.

Completion of basic body plan formation (3-5 days of incubation; H.H. stages 20-25)

TUNEL-positive branchial arches became most clearly observed at H.H. stage 20. The optic cup no longer contained TUNEL-positive cells, while the lateral surface of the lens and its adjacent epithelium were still apoptotic (Fig. 7 C,E). The pineal body contained increased numbers of TUNEL-positive cells (data not shown). In the trunk, TUNEL-positive cells in the ventral sclerotome and dermomyotome were sharply reduced, with only the dermomyotome remaining weakly apoptotic (Fig. 7F). Stainings which showed a metameric pattern (Fig. 7D) were frequently observed, mainly in the anterior trunk. Histological sections revealed TUNEL-positive mesenchymal cells distribute lateral to the somites between the dermomyotome and epidermis (Fig. 7G). The limb ectoderm and associated small numbers of mesenchymal cells are apoptotic at both anterior and posterior tips of the limb buds (Fig. 7 D,G).

Between H.H. stages 20-24/25, intense TUNEL-positive regions were confined to the limb buds (Fig. 7 B,J), tail bud, and the

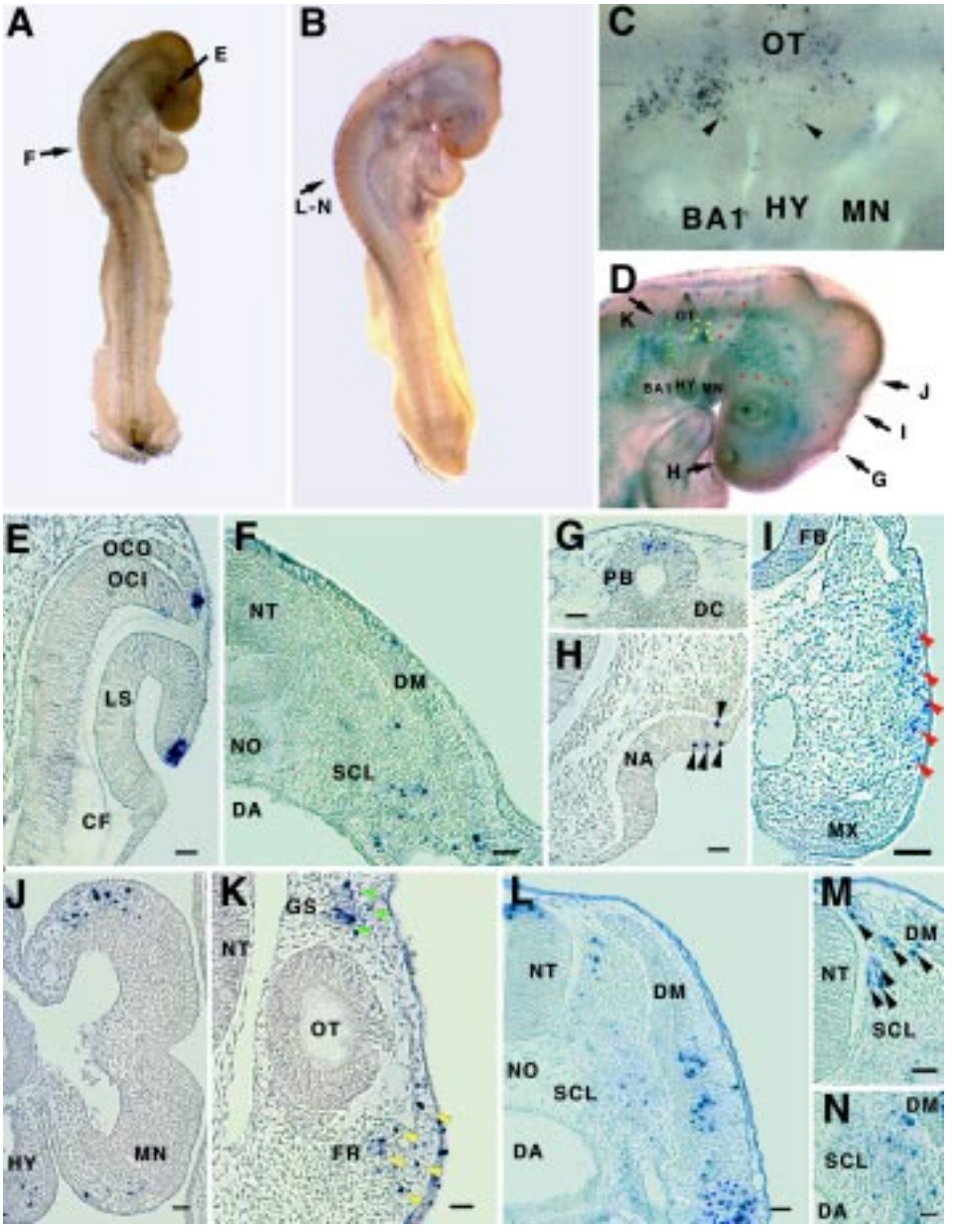

Fig. 6. Apoptotic cells as detected at late somitogenesis. *(A-D) Whole-mount-stained embryos. (A and B) Dorso-lateral views of embryos of stages 16* **(A)** *and 18* **(B)**. *Arrows indicate approximate level and direction of transverse sections shown in (E), (F), (L-N).* **(C)** *Stage 16, lateral view of higher magnification of A around the branchial region. Scattered TUNEL-positive cells (arrowheads) were first observed in branchial arches at this stage.* **(D)** *Stage 18, lateral view of higher magnification of (B) around the cranial region. Anterior (red), preotic (yellow) and postotic (green) stream-like staining of neural crest cells are most clearly visible at this stage. Similar colored arrowheads in (I) and (K) distinguish each stream. Arrows indicate approximate level and direction of sections shown in (G-K). (E-N) Sections of TUNEL-stained embryos.* **(E)** *Stage 16, optic level along the choroid fissure as indicated in (A).* **(F)** *Stage 16, anterior trunk as indicated in (A).* **(G)** *Stage 18, at the level of the pineal body as indicated in (D).* **(H)** *Stage 18, at the level of the nasal pit as indicated in (D).* **(I)** *Stage 18, forebrain level as indicated in (D).* **(J)** *Stage 18, a horizontal section through the pharyngeal arches as indicated in (D). Scattered TUNEL-positive cells were observed in both mandibular and hyoid arches.* **(K)** *Stage 18, parahorizontal section through the ventral otic vesicle with dorso-caudal at the top to show cell death in postotic (green) and preotic (yellow) streams (cf. (D)) in the positions of the presumptive glossopharyngeal nerve superior (GS) and facial nerve root (FR) ganglia.* **(L)** *Stage 18, anterior trunk region approximately at the level indicated in (B). Blue dotted circle; TUNEL-positive dense mesenchymal cell mass in the ventro-lateral portion of the somite.* **(M)** *Stage 18, anterior trunk region at the same somitic level as (L). TUNEL-positive neural crest cells (arrowheads) around the dorsal neural tube stream into the dorsal sclerotome.* **(N)** *Stage 18, a transverse section of the anterior trunk region at the same somitic level as (L). Numerous TUNEL-positive cells are seen within the ventral sclerotome. Scale bars, (E-H), (J-N), 20 μm; (I), 50 μm.*

lateral trunk, the latter in relation to closure of the body wall (Fig. 7J). In the limb buds, TUNEL-positive regions were mainly at the anterior and posterior borders (Fig. 7 B,J) in the regions of mesenchymal cell death (anterior necrotic zone, ANZ; posterior necrotic zone, PNZ) which appear at H.H. stage 25 (Saunders *et al.*, 1962) and is associated with morphogenesis of the limb buds. At H.H. stages 24-25, faint staining was still observed in optic (Fig. 7H), nasal (data not shown) and caudal branchial regions (Fig. 7I). Faint staining observed in the dorsal optic cup might relate to growth of the optic cup. The timing of the appearance of representative TUNEL-positive components during the morphogenetic period (H.H. stages 8-25) is summarized in Fig. 8. Table 1 contains a more detailed summary of TUNEL-positive components, including H.H. stages of maximal and minimal TUNEL-reactivity.

Discussion

We examined the temporospatial pattern of naturally occurring cell death in chick embryos between 0 and 5 days of incubation (H.H. stages 1-25) using the TUNEL labeling technique on both whole mount and serially sectioned embryos. Cell death occurred reproducibly at specific stages and regions during this morphogenetic phase of development. Following a brief discussion of the reproducibility and reliability of TUNEL labeling we discuss the temporospatial patterns of cell death and their significance for embryogenesis.

Reproducibly and reliability of TUNEL labeling for the detection of programmed cell death

The principle of TUNEL method is labeling DNA fragments, which accompany programmed cell death and are the most

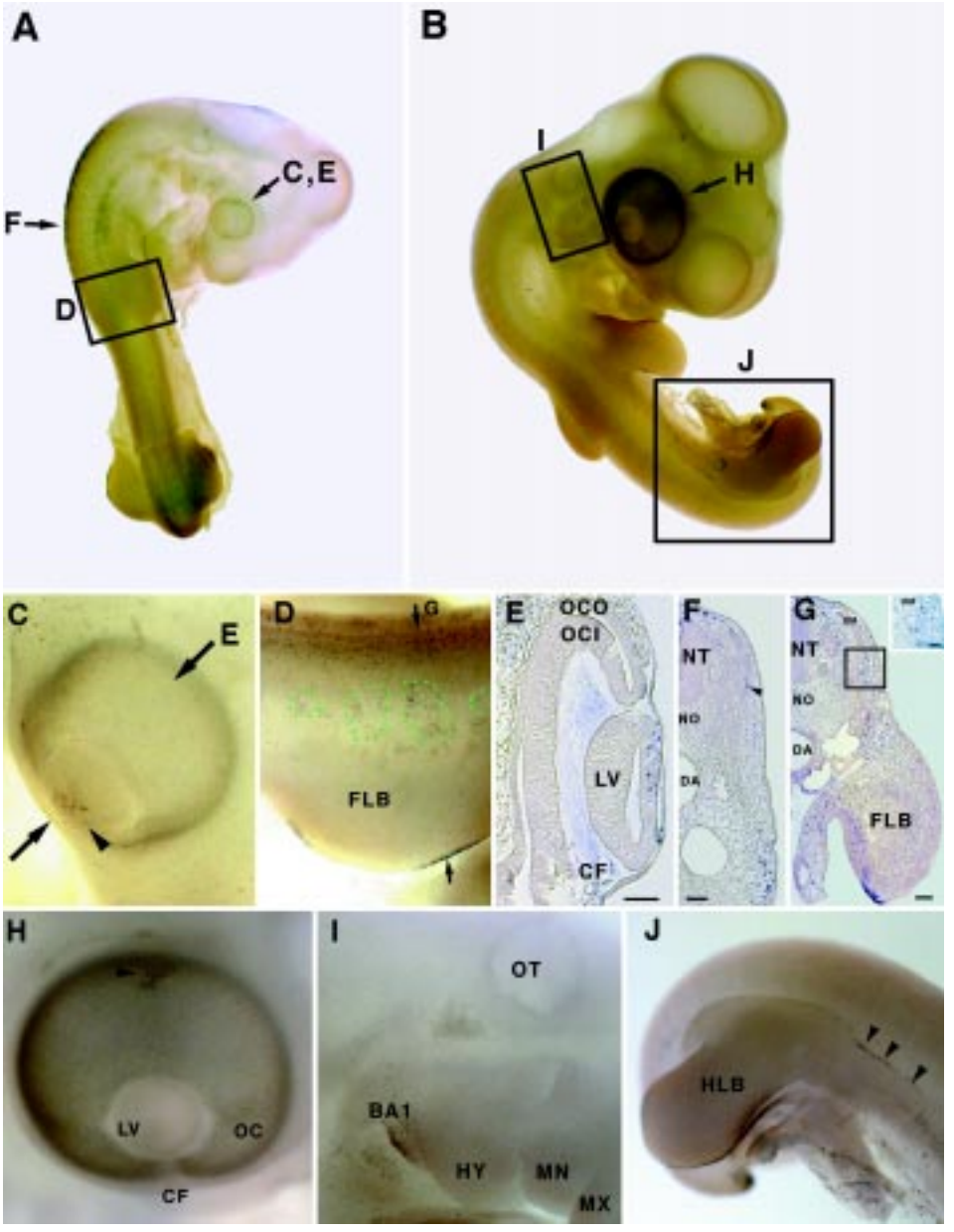

Fig. 7. Apoptotic cells detected at the period of completion of the basic body plan. *(A-D, H-J) Whole-mount-stained embryos. (E-G) Transverse sections of whole-mount-stained embryos. (A, B) Dorso-lateral views of whole-mount embryos at stages 20* **(A)** *and 24/25* **(B)**. *Arrows and boxes indicate the level and direction of transverse sections and higher magnification images shown in (C-F) and (H-J).* **(C)** *Stage 20, higher magnification image of the optic region. Arrows indicate level and direction of histological section shown in (E). Arrowhead indicates TUNEL-positive cells in the lateral portion of the lens vesicle.* **(D)** *Stage 20, higher magnification image of (A) at forelimb level. Arrows indicate level and direction of histological section shown in (G). Green dots outline a metameric pattern of TUNEL-positive cells.* **(E)** *Stage 20, a transverse section of the optic cup along the choroid fissure as indicated in (A) and (C). The lateral surface of the lens vesicle and its adjacent epithelium were still apoptotic.* **(F)** *Stage 20, a transverse section of the anterior trunk region as indicated in (D). Reduced numbers of TUNEL-positive cells (arrowhead) are seen in the somite.* **(G)** *Stage 20, a transverse section at the forelimb level as indicated in (D).* **(H)** *Stage 24/25, dorso-lateral view of higher magnification of the optic region. The lens no longer contains TUNEL-positive cells; however very faint staining appeared at the dorsal optic cup associated with growth of the optic cup (arrowhead).* **(I)** *Stage 24/25 lateral view of higher magnification of the branchial region.* **(J)** *Stage 24/25, dorso-lateral view of higher magnification of the posterior trunk region. TUNEL staining appeared along the ventro-lateral body wall in relation to closure of the body wall (arrowheads), and along the hindlimb bud. Apparent double lines of staining along the anterior border of the hind limb bud are due to a separation of the single band of staining. Scale bars: (E), 20 μm; (F), (G), 50 μm; (G) inset, 20 μm.*

characteristic features of cells undergoing apoptosis. It is known that small DNA fragments, known as Okazaki fragments, are synthesized at the phase of DNA duplication, which occurs only at the S-phase of the cell cycle (Alberts *et al.*, 1995). Even should such DNA fragments be detectable by the TUNEL method, so many adjacent cells would not be so synchronized at s-phase of the cell cycle to be recognized and detected as "TUNEL-positive".

Furthermore, in our results, TUNEL-positive regions did not always correlate with regions of higher cell proliferation. If Okazaki fragments are detected by this method, all tissues at the active morphogenetic phase (i.e., tissues with higher levels of cell proliferation) should be detected as TUNEL positive, since DNA duplication is closely related to cell division. For example, TUNEL-positive cells are more frequently observed in somites in older than in younger embryos; see our result in H.H. stage 11 and 14 whole-mount-stained embryos. Moreover, meaningful numbers of positive cells are not detected, with the exception of the anteromost tip of the neural plate at H.H. stage 7-8 embryos (see the result in H.H. stage 8 whole-mount-stained embryo), though they are at an active morphogenetic phase for both somitogenesis and neurogenesis. Identification of the same pattern of cell death in craniofacial regions of H.H. stage 11 embryos in our study, by Farlie *et al.* (1999) and by Lawson *et al.* (1999), reflects the reproducibly of the TUNEL method to detect apoptotic cells throughout the morphogenetic period of chick development.

Patterns of programmed cell death

The temporospatial distribution pattern we described in older embryos are consistent with and expand the result of past studies on cell death in early chick development which focused on gastrulation (Sanders *et al.*, 1997), sclerotome (Sanders, 1997) and

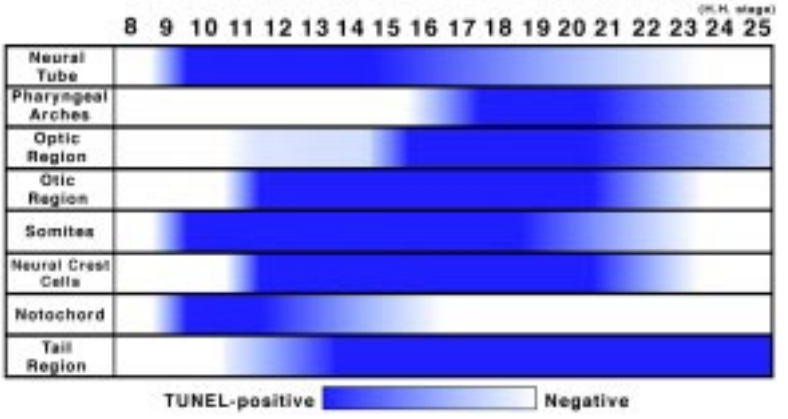

Fig. 8. Summary of the appearance of representative TUNEL-positive components during the morphogenetic period of chick development, H.H. stages 8-25.

hindbrain and associated neural crest cells (Farlie *et al*., 1999; Lawson *et al*., 1999) using TUNEL labeling.

Though the numbers are small, in our study TUNEL-positive cells were observed specifically, and for the first time, in the embryonic shield at H.H. stage 1. Cell death before gastrulation in avian embryos has not previously been reported. Initiation of avian gastrulation is defined as the formation of the primitive streak (Bellairs and Osmond, 1998). H.H. stage 1 corresponds to the pregastrula embryo. From the point of view of the onset of cell death, our result relates to the result obtained by Hensey and Gautier (1997, 1998), who showed that the apoptotic program in *Xenopus* was activated at the onset of gastrulation. They considered the cell death at gastrulation to be the random elimination of abnormal cells that had accumulated since the initiation of cleavage; cell death in *Xenopus* does not begin until after the mid-blastula transition. We are investigating the precise onset of TUNEL-positive cells before gastrulation in chick embryos.

Scattered TUNEL-positive cells were observed ubiquitously within embryos except in the region of the primitive streak at H.H. stage 3. At the head-process stage, TUNEL-positive cells were restricted to where head fold formation would occur at H.H. stage 6. Sanders *et al* (1997) — a good source for discussion of earlier literature — examined cell death in chick embryos during gastrulation and early neurulation (H.H. stages 4-6). Cell death, although widespread at these stages, was most evident in two regions: in the germinal crescent rostral to the embryonic axis; and laterally in the epiblast at the border of area pellucida and area opaca. We have extended this study by examining development before H.H. stage 4, finding that cell death is widespread at the onset of embryonic development but is excluded from the future primitive streak. The mechanism(s) that target cell death to extraembryonic cells or that protects future embryonic cells from removal by apoptosis at these early stages remain to be determined.

During early somitogenesis (H.H. stages 7-9), much of the staining was localized to the anteromost edge of the neural plate in the future forebrain, a site of active growth and morphogenesis. TUNEL-positive neural plate and notochord were first observed late in this period at H.H. stage 9. Otic and optic regions first became TUNEL-positive at mid somitogenesis (H.H. stages 11-14) in association with invagination of the otic and optic placodes. TUNEL-positive mesenchymal cells (neural crest cells) associated with the neural tube appeared in the trunk region. A TUNEL-positive population is found in the most caudal region of embryos at H.H. stage 11 may relate to initiation of tail bud formation. Apoptotic cells were distributed throughout the tail bud. Previously, cell death in the tail bud was described as beginning at H.H. stage 14 and as involved in remodeling the tail bud (Sanders *et al.,* 1986; Griffith *et al*., 1992). Our additional finding of cell death at H.H. stage 11 in the aggregation of cells that presages the tail bud indicates that removal of tail bud cells is one of the mechanisms regulating the size of the tail bud primordium. Apoptosis at later stages may have the additional function of preventing segmentation as suggested by Sanders *et al.* (1986).

TUNEL-positive cells appeared in relation to the formation of the secondary neural tube, tail and neural tube closure. Closure of the dorsal neural tube is facilitated by a zone of cell death within the neural folds and adjacent epithelium, a zone that becomes more focused as the region of fusion is approached. The extension of this zone into the epithelium adjacent to the neural folds (Fig. 4F), indicates that closure of the neural folds involves some remodeling of the immediately adjacent epithelium, i.e., that neural fold closure is not

TABLE 1

A SUMMARY OF THE TIMING OF THE DISTRIBUTION OF APOPTOTIC CELLS BETWEEN H.H. STAGES 1-25 WITH AN INDICATION OF THE STAGES OF MAXIMAL AND MINIMAL TUNEL STAINING

Structure	H. H. stages when apoptotic cells seen		
	Range	Maximum	Minimum
Embryonic shield	1	7 hours[a]	3 hours[a]
Headfold	5-6	(b)	(b)
Anterior neural plate (future forebrain)	7-8	(b)	(b)
Posterior open neural plate	7-8	(b)	(b)
Neural tube	9-22	14	22
Dorsal epidermis adjacent to neural tube	9-22	14	22
Closing neural tube	11-14	(b)	(b)
Secondary neural tube	14		
Floor plate	11-14	11	14
Brain			
forebrain	8-15	11-13	8, 14/15
midbrain	9-15	11-13	9, 14/15
hindbrain	9-22	9-15	16-22
fore-, mid-, hindbrain excluding rhombomere 4	11		
Cranial neural crest streams	16-19	18	16, 19
Pineal gland	18-20	(b)	(b)
Notochord	9-16	9-11	14-16
Otic placode/vesicle	11-23	11-20	23
Optic placode/vesicle	11-25	16-20	11-14, 25
Lens and adjacent epithelium	20-23	20	23
Nasal pit	18-25	(b)	(b)
Anterior intestinal portal	9-14	14	9-12
Somites	9-22	16-18	22
dermomyotome	14-20	18	14, 20-22
ventral sclerotome	14-18	18	14
Heart (outflow tract connection to the pharynx)	11	(b)	(b)
Pharyngeal arches	16-25	20	25
Tail bud primordium/tail bud	11-25	(b)	(b)
Limb buds: anterior and posterior necrotic zones	20-25	(b)	(b)
Lateral body wall	25		

(a) Given as hours of incubation, 3 hours being H.H. stage 1, 10 hours being gastrulation.
(b) No change in intensity of TUNEL reaction

a simple 'zipping-up' of neural ectoderm. TUNEL-positive cells distributed within the secondary neural tube did not show clear localization along dorso-ventral axis when compared with those in the primary neural tube. This suggests that the morphogenetic mechanism of secondary neural tube formation differs from that of primary neural tube formation, as pointed out recently in tail growth in embryonic mice (Hall, 2000). Hensey and Gautier (1998) described the pattern of cell death in *Xenopus* tail buds as less defined than the pattern seen in other tissues, coupling this less well defined pattern with the random cell death seen at gastrulation in *Xenopus*. An intriguing possibility is that secondary neurulation of the caudal region of vertebrate embryos — a process that occurs without organization of the caudal region into germ layers (Hall, 1998) — employs similar mechanisms of removal of dead cells to that seen during gastrulation, which is the phase of development when germ layers are established in all but the most caudal embryonic region. Given that secondary neurulation is a primary feature of vertebrate embryogenesis (Hall, 1998), we would expect similar mechanisms to exist in all vertebrates. Comparative analyses of primary and secondary neurulation (primary and secondary body formation), or of formation of germ layers and secondary neurulation across the vertebrates, is likely to yield valuable information on the evolution and/or conservation of mechanisms of cell death.

During late somitogenesis (H.H. stages 16-18), scattered TUNEL-positive cells were first observed in the branchial arches, while staining of the cranial neural tube became relatively faint compared to the previous stages, the major morphogenetic events associated with neurulation being completed. We showed that apoptosis in the branchial arches is prolonged, extending from H.H. stages 16 to 25. Therefore, continued removal of mesenchymal cells during growth is a normal feature of branchial arch development, as it was also shown to be during tail bud development. Similarly, apoptotic cells are associated with closure of the lateral body wall at H.H. stage 25. Thus, apoptosis is not limited to situations in which cells would be expected to die (such as body wall closure or fusion of the neural folds), but also is a feature of situations of rapid growth of specific regions at early stages in the development; cell death is a normal part of development. At completion of basic body plan formation (H.H. stages 20-25), intense TUNEL-positive regions were confined to sites involving morphogenesis and patterning, viz., the limb buds, tail bud, and the lateral body wall.

Neural crest cells emerge from the dorsal neural tube and migrate via characteristic pathways to give rise to particular cell types (reviewed in detail by Hall, 1999 and Le Douarin and Kalcheim, 1999). With respect to cell death in the hindbrain, Lumsden *et al.* (1991), Jeffs and Osmond (1992), Jeffs *et al.* (1992) and Graham *et al.* (1993) demonstrated that rhombomeres r3 and r5 are rhombomeres in which putative neural crest cells fail to migrate and in which neural crest cells undergo cell death following H.H. stage 11. We also identified apoptotic cells in r3 and r5 but not in r4 (Fig. 4A) and HNK-1-immunoreactive neural crest cells at the preotic (r4) level (Fig. 5A). Sechrist *et al.* (1993) and Birgbauer *et al.* (1995) showed that neural crest cells from r3 and r5 migrate into r2, r4 and r6 before migrating from the neural tube, i.e., that neural crest cells that originate in r3 and r5 do not undergo cell death. Indeed, cell death can be induced in odd-numbered rhombomeres, e.g., in response to exogenous *Msx-2* (Takahashi *et al.,* 1998). Furthermore, cell death also occurs in portions of the hindbrain from which neural crest cells actively migrate (Lawson and England, 1998). A subsequent study of the hindbrain between H.H. stages 12 and 15 by Lawson *et al.* (1999) showed that, while cell death before H.H. stage 12 is restricted to neural crest cells, after stage 12, both neural crest and neuroepithelial cells undergo cell death, the latter contributing to thinning of the roof of the hindbrain at H.H. stages 14/15. Farlie *et al.* (1999) revealed previously unreported variability in numbers and patterns of cell death in the hindbrain, the tendency being for elevated apoptosis at the boundary between r2 and r3.

We visualized three different streams of TUNEL-positive populations in the cranial region at H. H. stage 18. The origin and destination of these streams was highly consistent with the migratory pattern of cranial neural crest streams (Nishibatake *et al.,* 1987; Shigetani *et al.,* 1995). The most anterior population originated from the forebrain and midbrain extending towards the anterior branchial arches; another population was seen in the preotic region extending from the anterior rhombencephalon towards the hyoid arches. The most caudal stream was observed at the postotic region, and seems to be directed to the posterior branchial arches. TUNEL-positive cells in the postotic and preotic stream were observed at the sites of the root ganglion of the facial nerve (cranial nerve VII) and the superior ganglion of the glossopharyngeal nerve (cranial nerve IX). The ganglion for cranial nerve VII is derived from placodal and neural crest cells; that for cranial nerve IX is derived entirely from neural crest (Webb and Noden, 1993; Hall, 1999; Le Douarin and Kalcheim, 1999). Colocalization of these ganglia with streams of apoptotic neural crest cells was confirmed with HNK-1 antibody staining. HNK-1 has been extensively used to detect migratory neural crest cells and neural crest-derivatives among vertebrates (Vincent *et al.,* 1983; Vincent and Thiery, 1984; Bronner-Fraser, 1986; Erickson *et al.,* 1989; Sadaghiani and Vielkind, 1989, 1990; Laudel and Lim, 1993; Hou and Takeuchi, 1994; Hirata *et al.,* 1997, 1998 and references therein). The existence of streams of apoptotic neural crest cells at H.H. stage 18 when neural crest derivatives (ganglia) have already differentiated suggests, either that the migrating cells have fates other than ganglionic — survival of avian neural crest cells in migration pathways has been shown to be cell-fate dependent (Wakamatsu *et al.,* 1998) — and/or that excess, later migrating ganglionic cells, are removed by apoptosis. Before there removal by apoptosis, late migrating cells would facilitate regulation of ganglionic and/or other neural crest cell derivatives (Vaglia and Hall, 1999).

TUNEL-positive cells are scattered throughout the branchial arches, which contain substantial neural crest cells (Hall, 1999; Le Douarin and Kalcheim, 1999). In the trunk, TUNEL-positive cells were frequently observed in positions corresponding to neural crest cell migratory pathways; around the dorsal neural tube, within the sclerotome (ventral pathway) and between epidermis and dermomyotome (dorso-lateral pathway). The distribution of TUNEL-positive cells in the typical trunk neural crest migratory pathway was also shown in *Xenopus* development (Hensey and Gautier, 1997). Wakamatsu *et al.* (1998) demonstrated differential survival of neural crest cells in the lateral migration pathway in chick embryos depending on their subsequent cell fate, melanocyte precursors surviving but neuronal precursors being eliminated.

We detected sclerotome as TUNEL-positive at H.H. stage 18 and detected dermomyotome and presumptive early migratory neural crest cells as TUNEL-positive in the trunk region at stage 18.

However, at H.H. stage 20, only the dermomyotome remained TUNEL-positive in the trunk region. Sanders (1997), who examined cell death in sclerotome at two time periods (2.5 and 4 days of incubation) found that patterns of cell death at 2.5 days varied with the rostro-caudal level examined such that apoptotic cells were largely in the rostral half of the ventral sclerotome in somites 1-18, throughout the ventral sclerotome in somites 19-26 and were absent from somites 27-32. Sclerotomal cell death decreased sharply at 4 days, being primarily restricted to the caudal side of the fissure between adjacent somites. If we consider our result at H.H. stage 14 (i.e., that TUNEL-positive dermomyotome was observed only in the most anterior trunk) we can conclude that sclerotome is more TUNEL-positive in younger somites while dermomyotome is more TUNEL-positive in older somites, correlating with the earlier segregation of sclerotome from the somites. The dermomyotome in the most anterior trunk (to the 3 somitic level) contained small numbers of TUNEL-positive cells between 1.5 and 2 days, while in the caudal trunk the somitocoele and epithelial walls of the somites contained some apoptotic cells, although Sanders (1997) demonstrated that apoptotic cells within the somite are not derived from the somitocoele. Dermomyotome and ventral sclerotome in the anterior to mid-trunk (to the 20 somite level) contained apoptotic cells between 2 and 3 days. We therefore confirm and extend Sanders' finding that apoptotic cells in the dermomyotome are reduced during this period of development and show that apoptosis is no longer found in the ventral sclerotome, these changes occurring as early as 3 days of incubation.

In summary, apoptosis is involved at all stages of development examined: removing cells before formation of the primitive streak; at sites of active growth/invagination such as the anterior neural tube, otic and optic placodes, branchial arches and tail bud primordium; at sites of morphogenesis as in neurulation, branchial arch and lens formation; in association with active cell migration of neural crest and sclerotomal mesenchymal cells and in closure of the body wall; and in patterning organ rudiments as in the ANZ and PNZ during limb bud development. Apoptosis is not limited to sites of morphogenesis but is a feature of development from gastrulation onwards, and is as much a feature of sites of active growth/migrations as of sites of cell removal associated with morphogenesis and patterning. Apoptosis is regulated temporally and spatially, changing patterns reflecting phases of differentiation, growth and morphogenesis of individual tissues and organs. The existence of stable temporospatial patterns of cell death and their contribution to embryogenesis should be taken into account in analyses of embryo initiation, cell migration, cell differentiation, morphogenesis, growth and remodeling.

Materials and Methods

Experimental animals

Fertilized eggs were either used immediately or stored before incubation in a cold room at 10°C for no more than three days. Eggs were incubated at 36°C in a humidified incubator until they reached the appropriate stage. Embryos were staged into H.H. stages according to the criteria of Hamburger and Hamilton (1951), freed from their yolk, washed in phosphate-buffered saline (PBS, pH 7.4) and fixed in 4% paraformaldehyde (PFA) in PBS overnight at 4°C.

Whole-mount TUNEL staining

The *in situ* visualization technique of DNA fragmentation on whole-mount embryos was performed using the "*In Situ* Cell Death Detection Kit" AP® (Boehringer Mannheim, Germany), modified for whole-mount preparation. The kit uses non-radioactive labeling of apoptotic cells by DNA-end labeling; calf thymus terminal deoxynucleotidyl transferase (TdT) is used to incorporate fluorescein-12-2'-deoxyuridine-5'-triphosphate (fluorescein-dUTP) at the sites of 3'-OH termini in DNA. Fixed embryos were dehydrated through a graded series of methanol and stored in methanol at -20ºC. Stored embryos were rehydrated and washed with 2 mM levamisole in PBS, followed by soaking in a permeabilization solution (0.1% Triton X-100 in 0.1% sodium citrate) for 15 min.

Embryos were then washed for 10 min in distilled water, followed by 3 X 30 min in 0.1% Triton X-100 in 2 mM levamisole in PBS (PBTL) at room temperature. Embryos were transferred to TUNEL reaction mixture containing TdT and fluorescein-dUTP for 3 h at 37°C in the dark. Following 4 X 45 min washing in PBTL, the nonspecific binding of antibodies was blocked in 3% bovine serum albumin (Sigma, St. Louis, MO) in PBTL + 20% sheep serum (Sigma) overnight at 4°C in the dark. Specimens were then incubated with Converter-AP® solution containing peroxidase-labeled anti-fluorescein sheep Fab fragment for 3 h at room temperature followed by 4 X 45 min washings with PBTL. Staining was developed using 5-bromo-4-chloro-3-indolyl phosphate and nitro blue tetrazolium substrates. Whole mounts were photographed on a Zeiss TESSOVAR using a standard 35-mm camera. To confirm accessibility of enzyme and antibodies for whole-mount-staining, we carried out longer exposure (up to 2 days) in both labeling and antibody solutions, without influencing the results (data not shown).

Embedding and sectioning

Whole-mount-stained embryos were postfixed overnight at 4°C in 4% PFA in PBS. After dehydration in ethanol and embedding in Paraplast (Oxford Labware, St. Louis, MO), specimens were serially sectioned at 5 to 8 μm. Sections were dewaxed in Histoclear (Fisher Scientific, Pittsburgh, PA), mounted with Entellan (Merck, Darmstadt, Germany), observed under a Leitz ARISTOPLAN microscope and photographed.

Whole-mount staining of HNK-1 antibody

Rehydrated embryos were washed for 3 h in PBS, followed by 1 h in 0.1% Triton X-100 in PBS (PBST) at room temperature. Embryos were treated with 1% bovine serum albumin in PBST (BSA/PBST) overnight at 4°C to block nonspecific binding of primary antibodies. Specimens were then incubated for 2 days at room temperature in a solution of HNK-1 (CD57, Sigma) that had been diluted 1/40 fold with BSA/PBST. After 4 X 90 min washings with PBST, specimens were incubated in peroxidase-conjugated goat anti-mouse IgM (Sigma) diluted 1/100 fold with BSA/PBS overnight at 4ºC, followed by 4 X 90 min washings with PBST. The peroxidase reaction was performed in 20 ml of 0.05M Tris-HCl buffer (pH 7.6) containing 10 mg of 3-3'-diaminobenzidine (Sigma) and 2 μl of 30% hydrogen peroxide (Caledon Laboratories, Georgetown, Canada) for 30 min at room temperature. Whole mounts were photographed on a Zeiss TESSOVAR using a standard 35-mm camera.

Acknowledgments

We thank Drs. Carmel Hensey and Jean Gautier for useful suggestions for the procedures of whole-mount TUNEL staining, Drs. Scott Gilbert and Gary Schoenwolf for discussion about the definition of the gastrulation period in chick development, and Dr. Margaret Kirby for useful discussions and comments. M. H. acknowledges funding from the Suzuki Scholarship Foundation (Tokyo, Japan). B.K.H. acknowledges financial support from NSERC of Canada and the Killam Trust of Dalhousie University.

References

ALBERTS, B., BRAY, D., LEWIS, J., RAFF, M., ROBERTS, K. and WATSON, J.D. (1995). *Molecular biology of the Cell*, Third Edition. Garland Publishing, New York.

ANDERSON, J.A., LEWELLYN, A.L. and MALLER, J.L. (1997). Ionizing radiation

induces apoptosis and elevates cyclin A1-Cdk2 activity before but not after the midblastula transition in *Xenopus. Mol. Biol. Cell* 8: 1195-1206.

BELLAIRS, R. and OSMOND, M. (1998). *The Atlas of Chick Development.* Academic Press, San Diego.

BIRGBAUER, E., SECHRIST, J., BRONNER-FRASER, M. and FRASER, S. (1995). Rhombomeric origin and rostrocaudal reassortment of neural crest cells revealed by intravital microscopy. *Development* 121**:** 935-945.

BRONNER-FRASER, M. (1986). Analysis of the early stages of trunk neural crest migration in avian embryos using monoclonal antibody HNK-1. *Dev. Biol.* 115: 44-55.

CLARKE, P. (1990). Developmental cell death: Morphological diversity and multiple mechanisms. *Anat. Embryol.* 181: 195-213.

ELLIS, R.E., YUAN, J.Y. and HORVITZ, H.R. (1991). Mechanisms and functions of cell death. *Annu. Rev. Cell Biol.* 7: 663-698.

ERICKSON, C.A., LORING, J.F. and LESTER, S.M. (1989). Migratory pathways of HNK-1-immunoreactive neural crest cells in the rat embryo. *Dev. Biol.* 134: 112-118.

FARLIE, P.G., KERR, R., THOMAS, P., SYMES, T., MINICHIELLO, J., HEARN, C.J. and NEWGREEN, D. (1999). A paraxial exclusion zone creates patterned cranial neural crest cell outgrowth adjacent to rhombomeres 3 and 5. *Dev. Biol.* 213: 70-84.

GAVRIELI, Y., SHERMAN, Y. and BEN-SASSON, S. (1992). Identification of programmed cell death *in situ* via specific labeling of nuclear DNA fragmentation. *J. Cell Biol.* 119: 493-501.

GLÜCKSMANN, A. (1951). Cell deaths in normal vertebrate ontogeny. *Biol. Rev.* 26: 59-86.

GRAHAM, A., HEYMAN, I. AND LUMSDEN, A. (1993). Even-numbered rhomobmeres control the apoptotic elimination of neural crest cells from odd-numbered rhombomeres in the chick hindbrain. *Development* 119: 233-245.

GRIFFITH, C.M., WILEY, M.J. and SANDERS, E.J. (1992). The vertebrate tail bud: three germ layers from one tissue. *Anat. Embryol.* 185: 101-113.

HALL, B.K. (1998). Germ layers and the germ-layer theory revisited. Primary and secondary germ layers, neural crest as a fourth germ layer, homology and demise of the germ-layer theory. *Evol. Biol.* 30: 121-186.

HALL, B.K. (1999). *The Neural Crest in Development and Evolution.* Springer-Verlag, New York.

HALL, B.K. (2000). A role for epithelial-mesenchymal interactions in tail growth/morphogenesis and chondrogenesis in embryonic mice. *Cells Tissues Organs* 166: 6-14.

HAMBURGER, V. and HAMILTON, H.L. (1951). A series of normal stages in the development of the chick embryo. *J. Morphol.* 88: 49-92.

HENSEY, C. and GAUTIER, J. (1997). A developmental timer that regulates apoptosis at the onset of gastrulation. *Mech. Dev.* 69: 183-195.

HENSEY, C. and GAUTIER, J. (1998). Programmed cell death during *Xenopus* Development: A spatio-temporal analysis. *Dev. Biol.* 203: 36-48.

HIRATA, M., ITO, K. and TSUNEKI, K. (1997). Migration and colonization patterns of HNK-1-immunoreactive neural crest cells in lamprey and swordtail embryos. *Zool. Sci.* 14: 305-312.

HIRATA, M., ITO, K. and TSUNEKI, K. (1998). Significance of heterochronic differences in neural crest cell migration and sclerotomal development in evolution of the trunk body organization from agnathans to gnathostomes. *Zool. Sci.* 15: 903-912.

HOMMA, S., YAGINUMA, H. and OPPENHEIM, R.W. (1994). Programmed Cell death during the earliest stages of spinal cord development in the chick embryo: A possible means of early phenotypic selection. *J. Comp. Neurol.* 345: 377-395.

HOU, L. and TAKEUCHI, T. (1994). Neural crest development in reptilian embryos, studied with monoclonal antibody, HNK-1. *Zool. Sci.* 11: 423-431.

HURLE, J.M., ROS, M.A., GARCIA-MARTINEZ, V. and GANAN, Y. (1995). Cell death in the embryonic developing limb. *Scan. Microsc.* 9: 519-534.

IMOH, H. (1986). Cell death during normal gastrulation on the newt, *Cynops pyrrhogaster. Cell Differ.* 19: 35-42.

JACOBSON, M.D., WEIL, M. and RAFF, M.C. (1997). Programmed cell death in animal development. *Cell* 88: 347-354.

JEFFS, P. and OSMOND, M. (1992). A Segmented pattern of cell death during development of the chick embryo. *Anat. Embryol.* 185: 589-598.

JEFFS, P., JAQUES, K. and OSMOND, M. (1992). Cell death in cranial neural crest development. *Anat. Embryol.* 185: 583-588.

KERR, J.F., WYLLIE, A.H. and CURRIE, A.R. (1972). Apoptosis: A basic biological phenomenon with wide-ranging implications in tissue kinetics. *Br. J. Cancer* 26: 239-257.

LAUDEL, T.P. and LIM, T.-M. (1993). Development of the dorsal root ganglion in a teleost, *Oreochromis mossambicus* (Peters). *J. Comp. Neurol.* 327: 141-150.

LAWSON, A. and ENGLAND, M.A. (1998). Neural fold fusion in the cranial region of the chick embryo. *Dev. Dynam.* 212: 473-481.

LAWSON, A., SCHOENWOLF, G.C., ENGLAND, M.A., ADDAI, F.K. and AHIMA, R.S. (1999). Programmed cell death and morphogenesis of the Hindbrain roof plate in the chick embryo. *Anat. Embryol.* 200: 509-519.

LE DOUARIN, N.M. and KALCHEIM, C. (1999). *The Neural Crest*, Second Edition. Cambridge University Press, Cambridge, UK.

LEE, K.K.H., TANG, M.K., YEW, D.T.W., CHOW, P.H., YEE, S.P., SCHNEIDER, C. and BRANCOLINI, C. (1999). *gas2* is a multifunctional gene involved in the regulation of apoptosis and chondrogenesis in the developing mouse limb. *Dev. Biol.* 207: 14-25.

LUMSDEN, A., SPRAWSON, N. and GRAHAM, A. (1991). Segmental origin and migration of neural crest cells in the hindbrain region of the chick embryo. *Development* 113: 1281-1291.

MILLER, S.A. and BRIGLIN, A. (1996). Apoptosis removes chick embryo tail gut and remnant of the primitive streak. *Dev. Dynam.* 206: 212-218.

NISHIBATAKE, M., KIRBY, M.L. and VAN MIEROP, L.H.S. (1987). Pathogenesis of persistent truncus arteriosus and dextroposed aorta in the chick embryo after neural crest ablation. *Circulation* 75: 255-264.

NISHIKAWA, A. and HAYASHI, H. (1995). Spatial, temporal and hormonal regulation of programmed muscle cell death during metamorphosis of the frog *Xenopus laevis. Differentiation* 59: 207-214.

PEXIEDER, T. (1975). Cell death in the morphogenesis and teratogenesis of the heart. *Adv. Anat. Embryol. Cell Biol.* 51: 1-100.

SADAGHIANI, B. and VIELKIND, J.R. (1989). Neural crest development in *Xiphophorus* fishes: Scanning electron and light microscopic studies. *Development* 105: 487-504.

SADAGHIANI, B. and VIELKIND, J.R. (1990). Distribution and migration pathways of HNK-1-immunoreactive neural crest cells in teleost fish embryos. *Development* 110: 197-209.

SANDERS, E.J. (1997). Cell death in the avian sclerotome. *Dev. Biol.* 192: 551-563.

SANDERS, E.J., KHANE, M.K., OOI, V.C. and BELLAIRS, R. (1986). An experimental and morphological analysis of the tail bud mesenchyme of the chick embryo. *Anat. Embryol.* 174: 179-185.

SANDERS, E.J., TORKKELI, P.H. and FRENCH A.S. (1997). Patterns of cell death during gastrulation in chick and mouse embryos. *Anat. Embryol.* 195: 147-154.

SAUNDERS, J.W., GASSELING, M.T. and SAUNDERS, L.C. (1962). Cellular death in morphogenesis of the avian wing. *Dev. Biol.* 5: 147-178.

SCHOENWOLF, G.C. (1981). Morphogenetic processes involved in the remodeling of the tail region of the chick embryo. *Anat. Embryol.* 162: 183-197.

SECHRIST, J., SERBEDZIJA, G., SCHERSON, T., FRASER, S. and BRONNER-FRASER, M. (1993). Segmental migration of the hindbrain neural crest does not arise from its segmental generation. *Development* 118: 691-703.

SHIGETANI, Y., AIZAWA, S. and KURATANI, S.C. (1995). Overlapping origins of pharyngeal arch crest cells on the postotic hind-brain. *Dev. Growth. Differ.* 37: 733-746.

STACK, J.H. and NEWPORT, J.W. (1997). Developmentally regulated activation of apoptosis early in *Xenopus* gastrulation results in cyclin A degradation during interphase of the cell cycle. *Development* 124: 3185-3195.

TAKAHASHI, K., NUCKOLLS, G.H., TANAKA, O., SEMBA, I., TAKAHASHI, I., DASHNER, R., SHUM, L. and SLAVKIN, H.C. (1998). Adenovirus-mediated ectopic expression of *Msx2* in even-numbered rhombomeres induces apoptotic elimination of cranial neural crest cells *in ovo. Development* 125: 1627-1635.

VAGLIA, J.L. and HALL, B.K. (1999). Regulation of neural crest cell populations: occurrence, distribution and underlying mechanisms. *Int. J. Dev. Biol.* 43: 95-110.

VINCENT, M. and THIERY, J.P. (1984). A cell surface marker for neural crest and placodal cells: Further evolution in peripheral and central nervous system. *Dev. Biol.* 103: 468-481.

VINCENT, M., DUBAND, J.L. and THIERY, J.P. (1983). A cell surface determinant expressed early on migrating neural crest cells. *Dev. Brain Res.* 9: 235-238.

WAKAMATSU, Y., MOCHII, M., VOGEL, K.S. and WESTON, J.A. (1998). Avian neural crest-derived neurogenic precursors undergo apoptosis on the lateral migration pathway. *Development* 125: 4205-4213.

WEBB, J.F. and NODEN, D.M. (1993). Ectodermal placodes: Contributions to the development of the vertebrate head. *Am. Zool.* 33: 434-447.

Received: July 2000
Accepted for publication: October 2000